Chemistry
A European
Journal

Chemistry Europe
European Chemical Societies Publishing

Accepted Article

Title: A Proton-Responsive Pyridyl(benzamide)-Functionalized NHC Ligand on Ir Complex for Alkylation of Ketones and Secondary Alcohols

Authors: Mandeep Kaur, Noor U Din Reshi, Kamaless Patra, Arindom Bhattacherya, Sooraj Kunnikuruvan, and Jitendra K. Bera

To be cited as: *Chem. Eur. J.* 10.1002/chem.202101360

Link to VoR: https://doi.org/10.1002/chem.202101360

WILEY-VCH

A Proton-Responsive Pyridyl(benzamide)-Functionalized NHC Ligand on Ir Complex for Alkylation of Ketones and Secondary Alcohols

Mandeep Kaur,[a] Noor U Din Reshi,[a] Kamaless Patra,[a] Arindom Bhattacherya,[a] Sooraj Kunnikuruvan[b] and Jitendra K. Bera*[a]

Dedicated to Professor Wolfgang Kaim on the occasion of his 70th birthday

[a] Dr. M. Kaur, Dr. N. U D. Reshi, K. Patra, A. Bhattacherya, Prof. J. K. Bera
Department of Chemistry and Center for Environmental Sciences and Engineering
Indian Institute of Technology Kanpur, Kanpur 208016, India
E-mail: jbera@iitk.ac.in; @berachm
[b] Dr. S. Kunnikuruvan, School of Chemistry, Indian Institute of Science Education and Research Thiruvananthapuram, Vithura, Thiruvananthapuram 695551, India

Abstract: A Cp*Ir(III) complex (**1**) of a newly designed ligand L^1 featuring a proton-responsive pyridyl(benzamide) appended on N-heterocyclic carbene (NHC) has been synthesized. The molecular structure of **1** reveals a dearomatized form of the ligand. The protonation of **1** with HBF_4 in tetrahydrofuran gives the corresponding aromatized complex $[Cp^*Ir(L^1H)Cl]BF_4$ (**2**). Both compounds are characterized spectroscopically and by X-ray crystallography. The protonation of **1** with acid is examined by ^1H NMR and UV-vis spectra. The proton-responsive character of **1** is exploited for catalyzing *α*-alkylation of ketones and *β*-alkylation of secondary alcohols using primary alcohols as alkylating agents through hydrogen-borrowing methodology. Compound **1** is an effective catalyst for these reactions and exhibits a superior activity in comparison to a structurally similar iridium complex $[Cp^*Ir(L^2)Cl]PF_6$ (**3**) lacking a proton-responsive pendant amide moiety. The catalytic alkylation is characterized by a wide substrate scope, low catalyst and base loadings, and short reaction time. The catalytic efficacy of **1** is also demonstrated for the syntheses of quinoline and lactone derivatives via acceptorless dehydrogenation, and selective alkylation of two steroids, pregnenolone and testosterone. Detailed mechanistic investigations and DFT calculations substantiates the role of the proton-responsive ligand in the hydrogen-borrowing process.

Introduction

A protic ligand is capable of reversible interconversion between two electronically distinct states by gain or loss of a proton.[1–7] The ligand electronics controls proton transfer at proton-responsive unit and hydride transfer at metal center to/from a suitable acceptor/donor. The catalysts bearing these ligands effectively promote the reactions that involve hydride and proton management, such as (de)hydrogenation[1–11] and borrowing-hydrogenation.[12–16] The nature (acid-base properties) and the position/orientation of proton-responsive unit, along with the metal-hydricity,[17] are the key considerations to enable metal-ligand cooperation (MLC)[18–20] for efficient hydrogen delivery/acceptance.[21–24] Among the various designs explored, the protic catalysts based on the reversible (de)protonation of –OH/=O, $–CH_2$/=CH and –NH/=N motifs on pyridine,[25–27] bipyridine,[28–32] bipyrimidine[33] and azole-pyridine/pyrimidine[34–37] are particularly effective. Some of the representative examples that have been employed for catalyzing (de)hydrogenation and alkylation reactions are given in Scheme 1. Yamaguchi and co-workers reported a Cp*Ir(III) compound with bipyridonate ligand (Scheme 1a) for catalyzing dehydrogenative oxidation of alcohols under mild conditions.[32] The reversible proton transfer in this type of catalyst features an interconversion between the hydroxy/oxyanion (lactim/lactam) forms of the ligand. Li employed the same catalyst for α-alkylation of ketones with primary alcohols *via* borrowing-hydrogen methodology.[38] The same group also reported a double-protonated complex $[Cp^*Ir(6,6'\text{-}(OH)_2\text{-bpy})(H_2O)](OTf)_2$ (bpy = 2,2′-bipyridine) for N-alkylation of sulfonamides with alcohols in water.[39] Ke introduced a series of Cp*Ir(III) compounds bearing picolyl-functionalized NHC ligands incorporating a pendant –OH group for catalyzing base-free N-alkylation of aromatic amines and sulfonamides with primary alcohols.[40] Recently, we reported a proton-responsive annulated mesoionic carbene scaffold on Ir complex which shows lactam-lactim acid−base equilibrium (Scheme 1b).[41] Cyclometalated NHC-pyridyl platform where protonation/deprotonation takes place at the remote pyridine (N) site has been reported.[42] A lactam group installed on the NHC backbone is also known.[43]

Milstein revealed MLC involving dearomatization/aromatization ($–CH_2$/=CH) switch in pyridine-based pincer complexes bearing active methylene arm.[18,44] Several of these complexes are shown to activate challenging substrates or catalyze synthetic transformations.[45–51] A dearomatized Mn complex bearing a bipyridine-phosphine ligand (Scheme 1c) exhibits good catalytic activity in one-step synthesis of N-substituted hydrazones by coupling of alcohols with hydrazine *via* a partial borrowing-hydrogen path.[52] Protic imine moiety containing N atom, which has electronegativity intermediate to that of C and O, has also been incorporated in pyridine based pincer complexes (Scheme 1d)[53] and MLC involving deprotonation/protonation of the imine arm (–NH/=N)

with concomitant dearomatization/aromatization of the central pyridine ring has been elucidated.[5,54–61] Huang[5,53,54,62–67], Kirchner,[68–81] Sortais,[82,83] and Kempe[84–91] have studied these complexes and the presence of more acidic and stronger N–H bond appears to influence the catalytic efficacies of these complexes.[5,54,55,63,65,66] For example, the dearomatized "$PN^3(P)$" pincer complex given in Scheme 1d exhibits enhanced catalytic activity towards the homocoupling of amines as compared to a related methylene counterpart.[53]

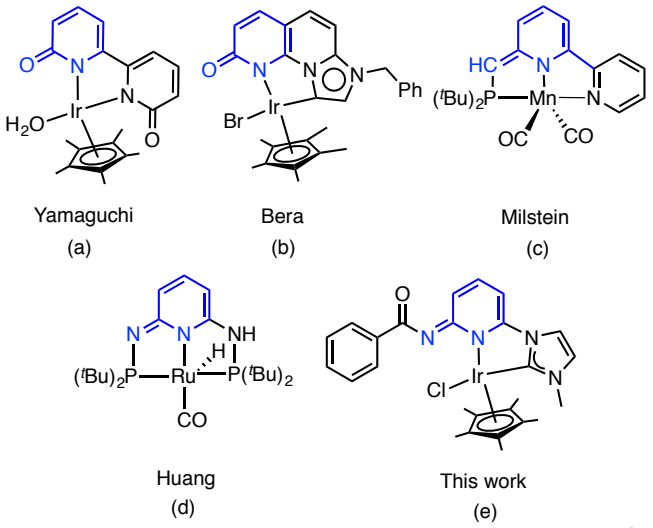

Scheme 1. Protic catalysts featuring proton-responsive functionalized pyridine scaffold.

Considering the need for designing new transition metal complexes bearing protic moieties, herein we report a pyridyl(benzamide)-functionalized NHC ligand and a dearomatized complex [Cp*IrL^{1}Cl] (**1**) (Scheme 1e) derived from it. The new ligand framework can exhibit MLC through a dearomatization-aromatization mode of action. The design features a chelating ligand that can strongly bind to metal ions which is desired to avoid catalyst decomposition via ligand dissociation.[27,92] Further, NHC being a strong σ-donor would promote the hydride transfer from the metal to a suitable substrate. The catalytic efficacy of **1** was evaluated in borrowing-hydrogen methodology for *α*-alkylation of ketones and *β*-alkylation of secondary alcohols using primary alcohols.[93–122] Apart from this, **1** was also employed for catalytic syntheses of quinoline and lactone derivatives and selective alkylation of two steroids pregnenolone and testosterone. Controlled experiments, mechanistic studies and density functional theory (DFT) calculations were performed to shed light on the role of proton-responsive unit in the catalysis.

Results and Discussion

Syntheses and Structures

The ligand precursor [**L**^{1}H$_2$]I was synthesized by refluxing N-(6-bromopyridin-2-yl)benzamide with imidazole in the presence of KOH and a catalytic amount of Cu_2O in dimethyl sulfoxide for 36 h, followed by quaternization with methyl iodide. The product was characterized by spectroscopic techniques and X-ray crystallography (See, SI). The ^{1}H NMR of [**L**^{1}H$_2$]I shows sharp singlets at δ 8.06 ppm and 10.2 ppm which are assigned to imidazolium N*CH*N and amide N–H protons, respectively. The ligand precursor [L^{2}H]PF_6 was synthesized following a literature procedure.[123]

[Cp*Ir(L^1)Cl] (1). A mixture of [**L**^{1}H$_2$]I, Ag_2O and [Cp*$IrCl_2]_2$ was stirred in dichloromethane at room temperature for 12 h. The resultant mixture was passed through a pad of celite and the filtrate was concentrated under reduced pressure. The addition of 10 mL of hexane led to the formation of a precipitate, which was washed with hexane (3 × 10 mL) and dried to afford **1** in 90% yield (Scheme 2).

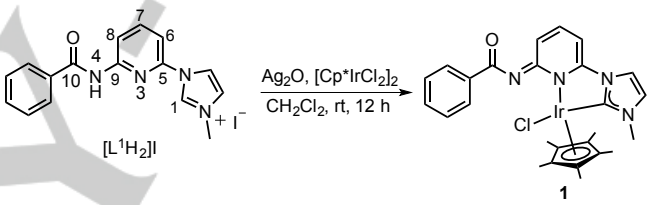

Scheme 2. Synthesis of **1**.

The ^{1}H NMR spectrum reveals the disappearance of the N*CH*N (C1-H) proton signal. The methyl protons of Cp* resonate at δ 1.64 ppm. The carbonyl and carbene carbons resonate at δ 173.1 and 166.4 ppm, respectively, in the ^{13}C NMR spectrum. The IR spectrum shows *ν*(CO) band at 1618 cm^{-1}. ESI-MS exhibits a signal at *m/z* = 605.2737 which is attributed to [**1** – Cl]$^+$.

The molecular structure of **1** confirms the chelate binding of **L**^{1} to Ir through carbene carbon (Ir1–C1 = 1.995(4) Å) and pyridyl nitrogen (Ir1–N3 = 2.142(3) Å) (Figure 1a). One Cp* and one chloride complete the piano-stool geometry around the metal center. The ∠N3–Ir1–C1 is 75.78(15)°. The dearomatized form of the ligand is revealed in the alternate short-long pattern of the C5–C6 (1.358(5) Å), C6–C7 (1.405(5) Å), C7–C8 (1.360(6) Å) and C8–C9 (1.424(5) Å) distances in the pyridine ring. The C9–N4(amide) bond (1.345(5) Å) is shorter as compared to pyridyl C9–N3 (1.366(5) Å). The carbonyl C10–O1 (1.241(5) Å) distance indicates double bond character.

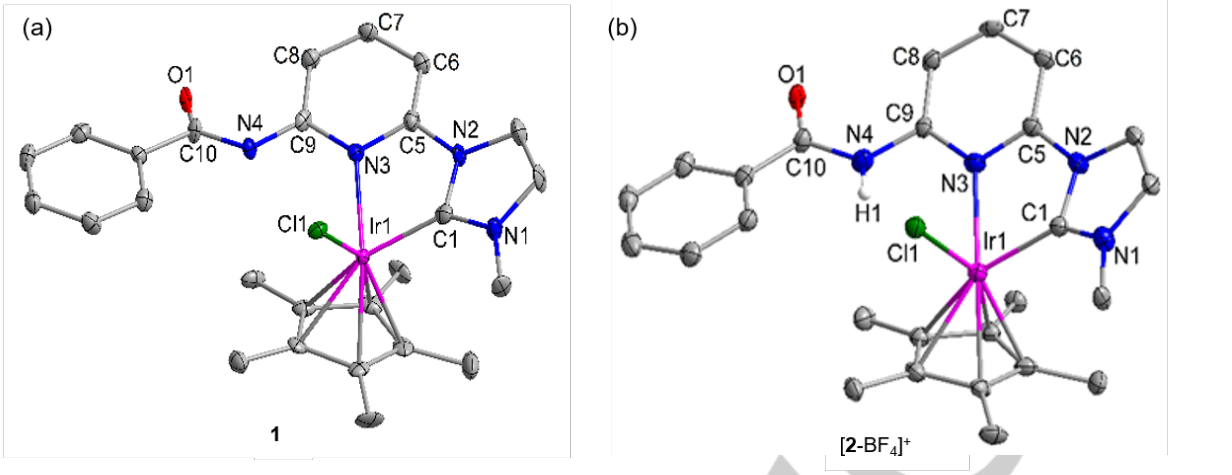

Ir1–C1 1.995(4), Ir1–N3 2.142(3), Ir1–Cl1 2.4313(9), N3–C5 1.360(5), C5–C6 1.358(5), C6–C7 1.405(5), C7–C8 1.360(6), C8–C9 1.424(5), N3–C9 1.366(5), C9–N4 1.345(5), N4–C10 1.360(5), C10–O1 1.241(5), N3–Ir–C1 75.78(15), C1–Ir1–Cl1 92.32(12), N3–Ir1–Cl1 93.64(9).

Ir1–C1 2.012(5), Ir1–N3 2.153(4), Ir1–Cl1 2.3897(13), N3–C5 1.341(7), C5–C6 1.376(7), C6–C7 1.391(8), C7–C8 1.359(8), C8–C9 1.386(8), N3–C9 1.354(7), C9–N4 1.388(7), N4–C10 1.372(8), C10–O1 1.213(8), C1–Ir1–N3 75.66(19), C1–Ir1–Cl1 89.79(15), N3–Ir1–Cl1 85.71(12).

Figure 1. Molecular structures of **1** and [**2**-BF_4]$^+$ with selected atoms labeled. Hydrogen atoms are omitted for clarity. Selected bond distances (Å) and angles (deg) are given below each structure.

[Cp*Ir(L^{1}H)Cl]BF_4 (2). The complex **1** was treated with one equivalent of HBF_4 in THF under N_2 atmosphere and stirred at room temperature for 2 h. The solvent was evaporated under vacuum and the resultant crude product was washed with 10 mL of diethyl ether which afforded **2** in 70% yield (Scheme 3).

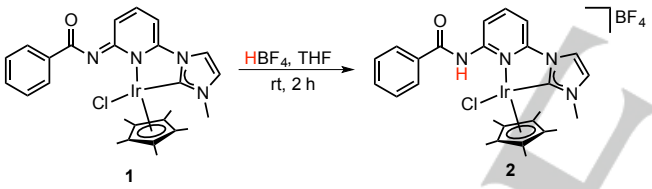

Scheme 3. Protonation of **1**.

In the ^{1}H NMR, the N–H proton signal appears at δ 10.08 ppm. A significant downfield shift (Δ(δ) = 0.9 ppm) for C8 proton is observed which indicates aromaticity of the pyridine ring is restored. The other pyridine protons also exhibit a downfield shift. Although the carbene carbon exhibits similar chemical shift (δ 166.5 ppm) to that of **1**, the carbonyl carbon is shifted upfield significantly (Δ(δ) 8.3 ppm). The C=O band is shifted to a higher frequency by 76 cm^{-1}. ESI-MS exhibits a signal at *m/z* = 641.1579 which is attributed to [**2** - BF_4]$^+$. The molecular structure of the cationic unit of **2** is similar to that of **1** except that the amide N is protonated and the pyridine ring is aromatized (Figure 1b). The reversal of the long/short C9–N3/C9–N4 bonds in **1** to a short (1.354(7) Å /long (1.388(7) Å) pattern in **2** indicates the aromatization of the pyridine ring. The Ir1–C1 and Ir1–N3 distances are 2.012(5) Å and 2.153(4) Å, respectively. The C10–O1 bond length in **2** (1.213(8) Å) is slightly shorter than **1** (1.241(5)), which is consistent with IR values.

[Cp*Ir(L^2)Cl]PF_6 (3). To emphasize the role of the proton-responsive unit in catalytic reactions, we also synthesized a control compound **3** where the amide side-arm is absent.[124,125] Complex **3** was characterized by various spectroscopic techniques and single crystal X-ray crystallography (see, SI).

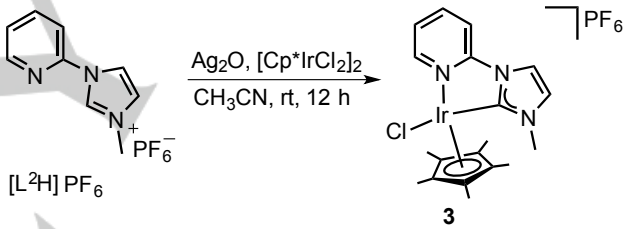

Scheme 4. Synthesis of **3**.

Protonation of 1

To authenticate the proton-responsive nature of the pendent amide unit, the protonation of **1** was studied. The gradual addition of trifluoroacetic acid to a solution of **1** in $CDCl_3$ was followed by ^{1}H NMR. A signal appeared at δ 10.02 ppm, which increased in intensity with the addition of acid, indicating the protonation of **1** (see, SI). The conversion was also monitored by UV-vis spectroscopy. A solution of **1** in acetonitrile exhibits absorption bands at 380 nm, 315 nm and 270 nm which can be assigned to metal to ligand charge transfer (MLCT) and/or ligand-centered (LC) transitions (Figure 2).[28,126,127] A gradual addition of trifluoroacetic acid to this solution resulted in a steady decrease in the intensity of the low energy band at 380 nm, which finally disappeared. Concomitantly, the intensity of bands at 315 nm and 270 nm increased. After several additions, the appearance of an isosbestic point was observed, that supports solution phase equilibrium between deprotonated and protonated forms. The changes in the UV-vis spectrum upon the addition of acid are indicative of protonation at the proton-responsive unit. [8,28,126–130] Both UV-vis and ^{1}H NMR results suggested the proton-responsive character of the ligand.

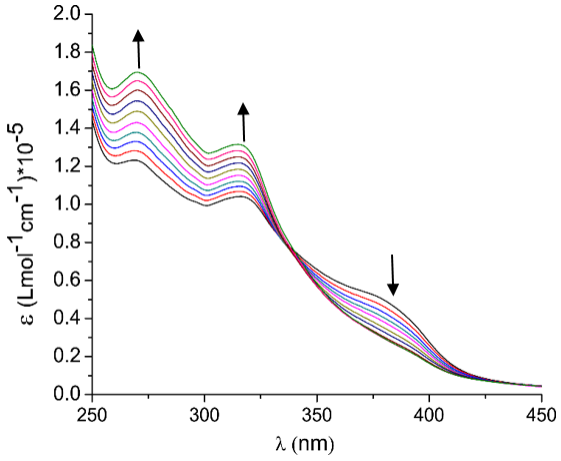

Figure 2. UV-Vis titration of **1** with CF_3COOH.

Catalytic Study

The catalytic efficacy of Cp*Ir(NHC) complexes has been demonstrated for a wide variety of reactions including transfer hydrogenation of ketones and imines,[131] cross-coupling of alcohols and amines,[132] benzylation of arenes,[133] and reductive amination.[41] In light of these reports, and recognizing that proton-responsive complexes are suited for catalyzing hydrogen-related reactions, the catalytic efficacy of **1** was evaluated for *α*-alkylation of ketones and *β*-alkylation of secondary alcohols using primary alcohols as alkylating agents.[93–122] Alcohols are attractive green and sustainable alkylating agents as compared to mutagenic alkyl halides and sulfonate esters employed in conventional alkylation methods.[134] Besides, the only by-product is water. These tandem reactions proceed via dehydrogenation of alcohol via hydride and proton transfer to a catalyst, followed by the reduction of the cross-aldol condensation product with hydrogen (hydride and proton) stored at the catalyst. We argued that complex **1** could effectively dehydrogenate alcohol to generate the hydrogenated form of the catalyst featuring a nucleophilic hydride at metal center and a proton on ligand amide moiety. Subsequently, both the hydridic and protic hydrogen atoms could be transferred to the unsaturated condensation product.

α-alkylation of ketones with primary alcohols

Initially, the *α*-alkylation of acetophenone with benzyl alcohol was tested using 5 mol% of **1** and 10 mol% of KOH in toluene at 130 °C, and a quantitative conversion to the corresponding product was obtained in 30 min (see SI for optimization study). Lowering catalyst loading to 0.05 mol% did not affect the yield of the product significantly and a high value of TOF (3880 h^{-1}) was achieved, though the further reduction in catalyst loading decreased the yield. The use of Cs_2CO_3 and NaOH instead of KOH afforded 98% and 94% yields of the product, respectively, whereas NaOAc, K_2CO_3 and DABCO were ineffective. In the absence of a base, less than 10% of the product was obtained. No significant change in conversion was observed when the reaction was carried out in DMSO but the use of *p*-xylene and 1,4-dioxane as solvents was detrimental to the catalytic activity. The dramatic effect of the base is likely due to its role in the removal of chloride from the precatalyst to generate a catalytically active species. The aromatized complex **2** afforded similar catalytic activity as that of **1** (see Supporting Information). Noticeably, when catalyst **3** was used under optimized conditions, only 20% yield of the alkylated derivative was obtained after 2 h. The significantly higher catalytic activity of complex **1** as compared to that of complex **3** highlights the vital role of the proton-responsive unit to facilitate the catalytic reaction. A range of primary alcohols and ketones was selected to examine the substrate scope of the protocol under optimized conditions. Benzyl alcohols having electron-donating methyl and methoxy substituents were effectively transformed into the corresponding *α*-alkylated products in high yields (85–90%, Table 1 entries 4b, 4c). The fluorine substituted benzyl alcohol afforded the desired product in 80% yield (entry 4d). The transformation of 2-naphthalenemethanol, heteroaromatic as well as aliphatic alcohols proceeded smoothly and their corresponding derivatives were obtained in high yields (70–91%, entries 4e–4l). Acetophenone derivatives bearing both electron-donating and electron-withdrawing groups such as methoxy, methyl, chloro and bromo afforded the corresponding *α*-alkylated derivatives with good to excellent yields (72–96%, Table 2 entries 5a–5h). The *α*-alkylated derivatives of 2-acetylnaphthalene and tetralone were obtained in 70 and 78% yields, respectively (entry 5i and 5j). The cyclic ketones furnished the respective products in 70–74% yields (entries 5k–5l).

Table 1. *α*-alkylation of acetophenone with various primary alcohols. [a]

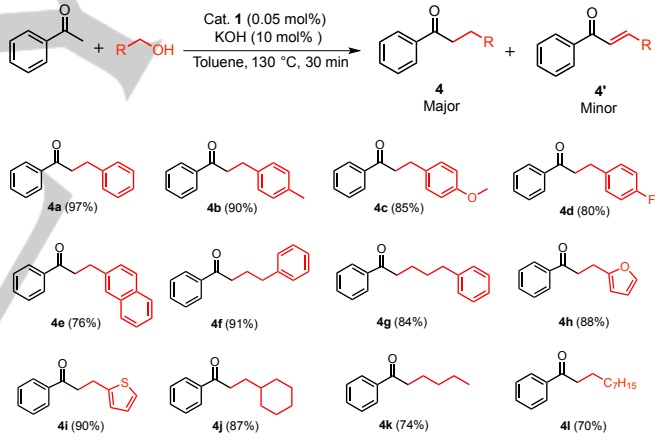

[a] Primary alcohol (4.16 mmol), acetophenone (4.16 mmol), **1** (0.05 mol%), KOH (10 mol%), toluene (5 mL), 130 °C. Yields determined by GC-MS analysis using n-dodecane as an internal standard. Traces (<2%) of the minor product were detected.

Table 2. *α*-alkylation of various ketones with benzyl alcohol. [a]

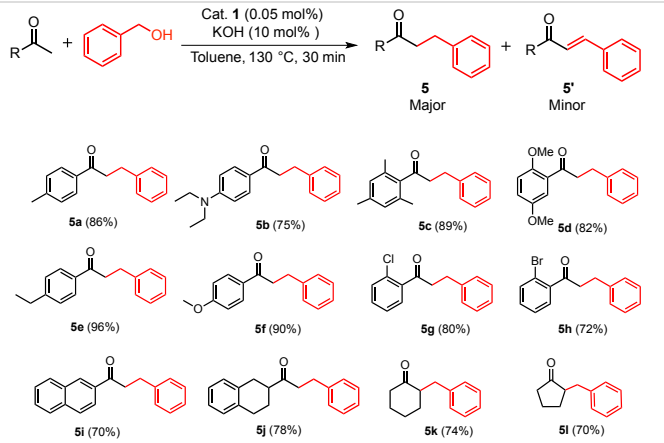

[a] Reaction conditions are the same as given in Table 1.

Table 3. *β*-alkylation of secondary alcohols with primary alcohols. [a]

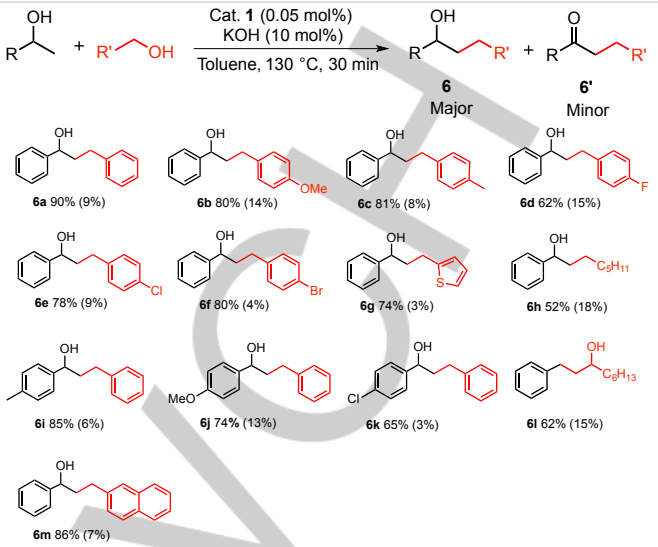

[a] Reaction conditions are the same as given in Table 1. Yieds of the minor products are given in parenthesis.

β-alkylation of secondary alcohols using primary alcohols

We then evaluated the efficacy of **1** for more challenging alkylation of secondary alcohols. The reaction of 1-phenylethanol with benzyl alcohol was conducted under optimized conditions as used for *α*-alkylation of ketones and the corresponding *β*-alkylated alcohol was formed selectively with TOF 3600 h^{-1}, along with a trace amount of *α*-alkylated ketone. The reaction proceeded smoothly with a series of electronically diverse primary and secondary alcohols depicted in Table 3. The *β*-alkylation of 1-phenylethanol using benzyl alcohol bearing electron-rich methoxy and methyl substituents afforded the corresponding alkylated products selectively in 80 and 81% yields, respectively (entries 6b,6c). The electron-deficient benzyl alcohols bearing fluoro, chloro and bromo substituents furnished the corresponding *β*-alkylated secondary alcohols in 62–80% yields (entries 6d–6f). The heterocyclic alcohol 2-thiophenemethanol was successfully converted to the desired product with 74% yield (entry 6g). A lower yield (52%) of the desired product was obtained using an aliphatic alcohol 1-hexanol (entry 6h). The substrate scope was also extended to electron-rich and electron-deficient secondary alcohols, which converted to the corresponding *β*-alkylated derivatives selectively (65–85%, entries 6i–6k). 2-octanol gave the desired product with 62% yield (entry 6l). In addition, 2-naphthalenemethanol resulted in the corresponding desired product with a high yield (86%, entry 6m).

A comparison of the performances of reported proton-responsive catalysts was made (see, Scheme S2). It is apparent that **1** exhibits better catalytic efficacy in terms of lower base loading and higher TON and TOF values for both α-alkylation of ketones[38,110,121,135–138] and β-alkylation of secondary alcohols[87,94,104,106,139].

Synthesis of quinoline and lactone derivatives

Quinolines are recognized as an important class of heterocyclic compounds because of their wide application in pharmaceuticals and materials.[140–145] We explored the utility of **1** for catalyzing one-pot synthesis of quinoline and lactone derivatives as shown in Tables 4 and 5. The substrate scope for quinoline synthesis using 2-aminobenzyl alcohol was elaborated for substituted acetophenones (entries 7a–7c) as well as 2-acetylnaphthalene (entry 7d) and the corresponding quinoline derivatives were obtained in high yields after 12 h (70–84%). Apart from aromatic ketones, 2-octanone also resulted in the formation of the corresponding quinoline derivative with a moderate yield 65% (entry 7e). Similarly, dehydrogenative lactonization of different diols was successfully achieved employing **1** as shown in Table 5 (8a–8e).[146,147]

Table 4. Synthesis of quinolines via annulation of 2-amino-benzyl alcohol with various ketones.[a]

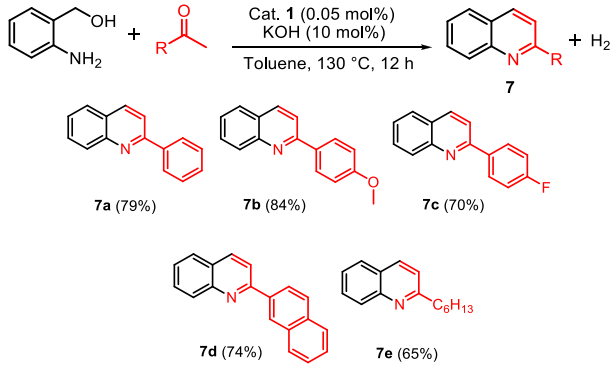

[a] Time 12 h, other conditions are the same as given in Table 1.

Table 5. Synthesis of lactones using diols. [a]

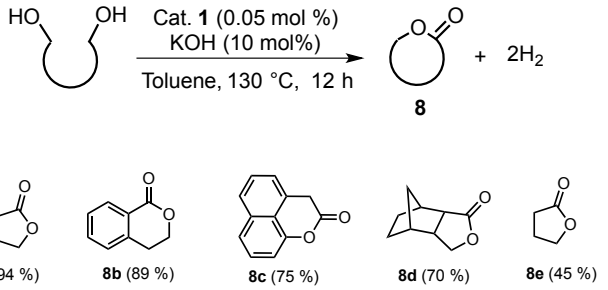

[a] Time 12 h, other conditions are same as given in Table 1.

Selective alkylation of steroids

The selective functionalization of steroids like pregnenolone and testosterone has drawn significant attention to explore structure-activity relationship (SAR) studies. Catalyst **1** was examined for the selective *α*-alkylation of both of these steroids at carbon atom adjacent to carbonyl group by using benzyl alcohol and 2-thiophenemethanol. The use of 1 mol% of **1** and 10 mol% KOH at 130 °C in toluene afforded the alkylated derivatives of pregnenolone (9a,b) and testosterone (9c,d) with 40–57% yield in 24 h (Scheme 5).

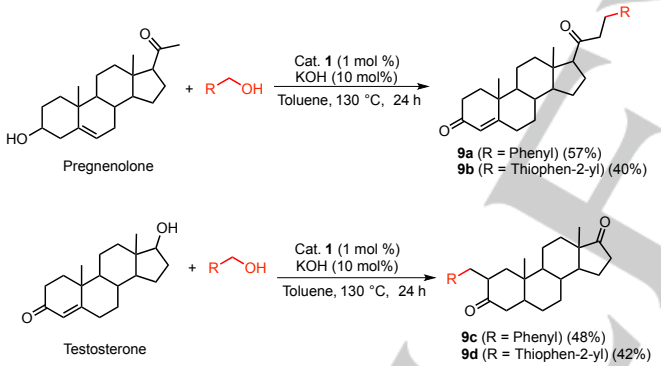

Scheme 5. *α*-alkylation of pregnenolone and testosterone using benzyl alcohol and 2-thiophenemethanol.

Reaction Profiles

The time-dependent product distribution of *α*- and *β*-alkylation is given in Figures 3a and 3b, respectively. The amounts of 1-phenylethanol and benzyl alcohol gradually decreased with time, and concurrently the amount of 1,3-diphenylpropan-1-ol is increased. Less than 2% of 1,3-diphenylpropan-1-one was detected throughout the reaction. The complete consumption of reactants takes place in 30 min. The reaction profile of *β*-alkylation shows a similar variation of the substrate and product amounts along with the formation of a small amount of 1,3-diphenylpropan-1-one (<10%).

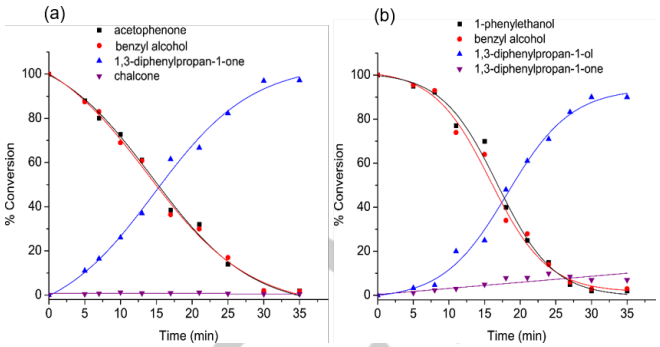

Figure 3. Reactions profiles under optimized conditions: (a) *α*-alkylation of acetophenone with benzyl alcohol; (b) *β*-alkylation of 1-phenyl ethanol with benzyl alcohol. Conversions were determined by GC-MS analysis.

Mechanistic Investigations

Proposed mechanism

We offer a mechanism for the alkylation reaction based on control experiments, deuterium labeling, DFT studies and taking earlier reports[96,99,100,102,103] into consideration (Scheme 6). It is presumed that initially a catalytically active species **I** is generated by the reaction of precatalyst **1** with KOH. The formation of **I** likely proceeds via a metal-hydroxide/alkoxide intermediate, followed by the release a H_2O/alcohol molecule on protonation. The reaction of an alcohol with **I** gives the corresponding carbonyl compound and the hydrogenated catalyst **II**. To validate the formation of intermediate **II**, a mixture of **1**, benzyl alcohol and $TlPF_6$ was heated at 45 °C in $CDCl_3$ in an NMR tube and the reaction was followed by ^1H NMR spectroscopy. After 5 min. the appearance of new signals at δ 10.1 ppm and δ -6.5 ppm was observed which is attributed to N–H and Ir–H protons, respectively. The downfield shift for pyridine C8 proton (Δ(δ) = 0.9 ppm) indicated the aromatization of the ring. The appearance of a signal at δ 9.8 ppm suggests the formation of aldehyde. Finally, the ligand-promoted 1,4-addition of N–H proton and Ir–H hydride to the *α,β*-unsaturated ketone,[148] which is generated by the base-catalyzed aldol condensation, affords *α*-alkylated ketone, regenerating catalytic species **I**.

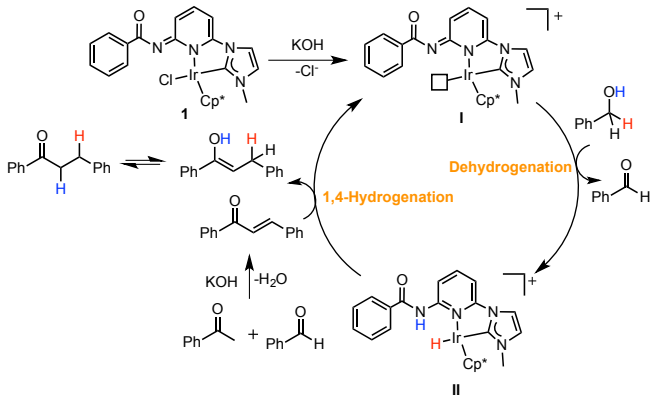

Scheme 6. Proposed reaction mechanism for α-alkylation of ketones.

Control experiments

Several control experiments were performed to gain insight into the possible steps in this transformation. Subjecting only benzyl alcohol to the catalytic conditions in the absence of any coupling partner (hydrogen acceptor), afforded benzaldehyde with the evolution of H_2 (Schemes 7a). The evolved H_2 gas was identified and measured.[149] To authenticate the borrowing-hydrogen pathway, *α,β*-unsaturated ketone (chalcone) was generated[109] and reacted with benzyl alcohol or 1-phenylethanol to afford the corresponding saturated ketone (Schemes 7b). These results show that **1** can effectively catalyze the transfer of hydrogen from the starting alcohols to C=C bond of the condensation product (chalcone). The *β*-alkylation of secondary alcohol proceeds via a saturated ketone intermediate (see, Supporting Information). To substantiate this assertion, a saturated ketone was reacted with alcohol resulting in the formation of the corresponding alcohol in 92% yield (Scheme 7c).

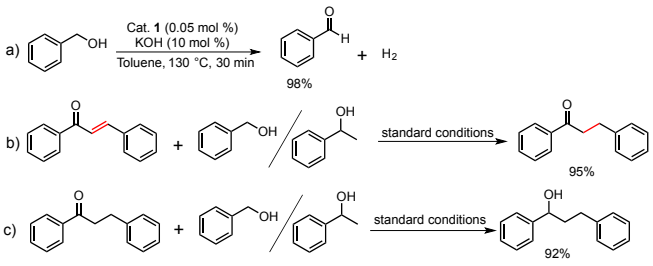

Scheme 7. Control experiments.

Deuterium-labeling experiments

The alkylation of acetophenone using benzyl alcohol [*α,α*-D_2] ($PhCD_2OH$) under optimized conditions led to the formation of the product with 95% deuterium incorporation at *β*-position and 2% deuterium incorporation at *α*-position (Scheme 8a). The high and low deuterium content at *β*- and *α*-positions, respectively, indicates that the reaction does not proceed via classical dihydride mechanism where similar deuterium incorporation is expected.[150–152] The alkylation of acetophenone using benzyl alcohol [*α,α*-D_2] ($PhCD_2OH$) catalyzed by **3** with no proton-responsive unit led to 70% deuterium incorporation at *β*-position and 15% deuterium incorporation at *α*-position (Scheme 8b). The reaction of benzyl alcohol [*α,α*-D_2] with 1-phenylethanol afforded the product with higher deuterium incorporation at *α* (75%) and *γ* (65%) positions as compared to *β*-position (10%) (Scheme 8c). The deuterium incorporation is significantly less with $PhCH_2OD$ having exchangeable single deuterium (Scheme 8d). The deuterium experiments are consistent with a 1,4-addition of H_2 to chalcone and indicate the involvement of both the metal and the participating ligand in the transfer-hydrogenation pathways (Scheme 6).[107] The results obtained with **1** are similar to those reported using Mn[137] and Fe[110] bifunctional catalysts. In contrast, a Co-catalyzed alkylation of acetophenone with secondary alcohol led to a comparable deuterium incorporation at both *α*- and *β*-positions owing to either reversible steps or a deuterium/hydrogen scrambling on the Co complex.[135]

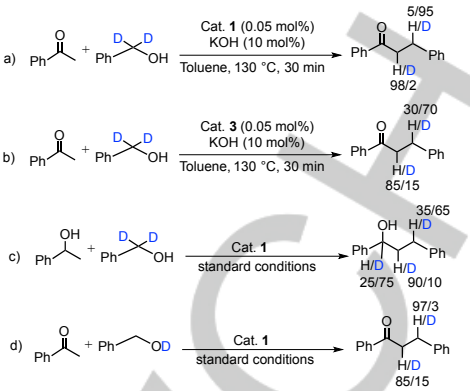

Scheme 8. Deuterium labeling experiments.

DFT studies

To corroborate the proposed mechanism, DFT calculations were performed for the **1**-catalyzed alkylation of acetophenone using benzyl alcohol as a model reaction. The calculations were performed using M06 hybrid meta-GGA functional.[153] LanL2DZ basis set by Hay and Wadt with effective core potentials[154] was used for Ir and 6-31+G(d,p) basis set was used for other atoms.[155,156] Technical details of the computations are provided in the experimental section.

Two limiting mechanistic scenarios can be considered for the transformation in hand: outer-sphere bifunctional pathway and inner-sphere *β*-H elimination pathway.[157,158] The free energy profile and the optimized structures along the bifunctional pathway are given in Figures 4 and 5, respectively, whereas the same along the inner-sphere path are given in the Supporting Information. For either route, it is presumed that chloride dissociates from **1** to generate catalytically active species **A**. The formation of **A** from **1** is an endothermic process (ΔG~43 kcal mol^{-1}). Along the bifunctional route, **A** reacts with benzyl alcohol to form a hydrogenated adduct **B.** The transition state (**TSAB**) for this step involves a synchronous transfer of hydride to Ir (Ir–H1=1.75 Å, C3–H1=1.32 Å) and proton to amide N (N1–H2=1.28 Å, O1–H2=1.20 Å). The Gibbs free energy barrier for this step is 20 kcal mol^{-1}. **B** was found to have stabilizing H2···O2 (2.44 Å) and H3···O2 (2.24 Å) interactions. The hydrogenation of the condensation product occurs in two steps. Initially, the hydride from Ir–H is transferred to *β*-carbon of chalcone, to form **C** via **TSBC**, with a free energy barrier of 27 kcal mol^{-1}. The species **C** features Ir–O2 (2.13 Å) bond, and is further stabilized by H2···O2 (1.91 Å) and H3···O2 (2.42 Å) interactions. Subsequently, **C** undergoes protonation at carbonyl oxygen of chalcone by –NH proton via **TSCA** to form an enol product and the cycle is completed. The Gibbs free energy barrier for this step is 17 kcal mol^{-1}.

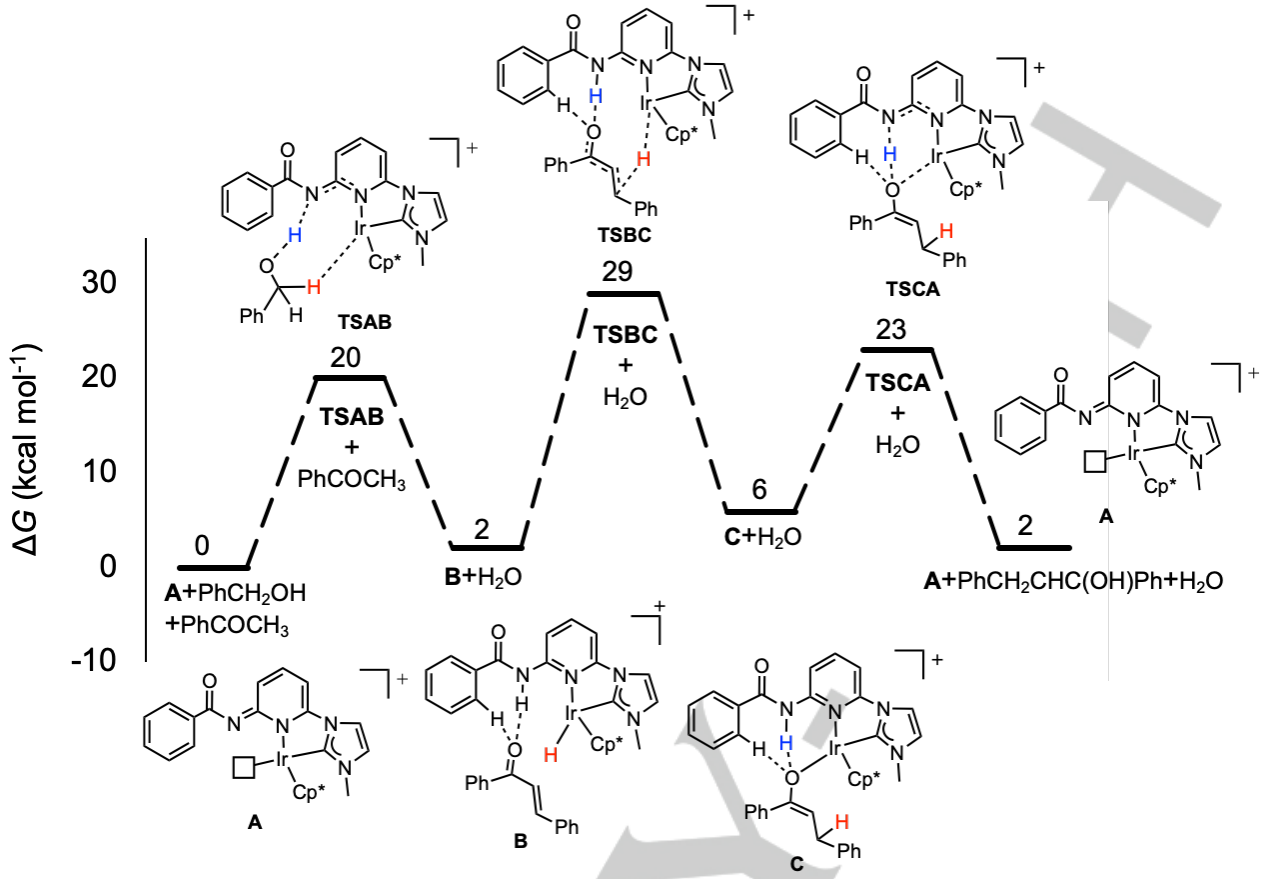

Figure 4. Free energy profile for the alkylation along the outer-sphere bifunctional pathway.

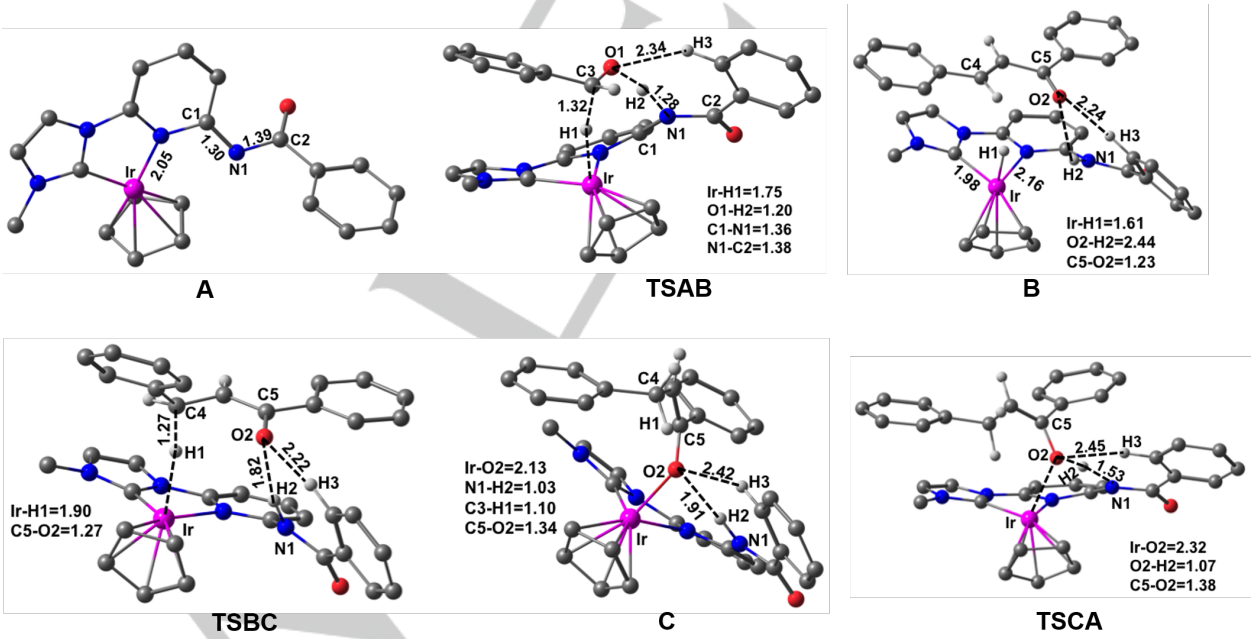

Figure 5. Optimized structures along the outer-sphere bifunctional pathway with important distances (in Å) labeled. For clarity, the methyl groups in Cp* and hydrogens on the five- and six-membered rings are not shown. Atom color codes: Ir(magenta), C(grey), N(blue), O(red), H(white).

Our attempts to identify a synchronous transition state for the hydrogenation step failed and ended up in structures similar to either of the transition states (**TSBC** or **TSCA**). It is likely due to the spatial disposition of Ir-H/N-H units not suited to deliver H^-/H^+ to chalcone in a concerted manner. In contrast, Renaud and co-workers obtained a synchronous transition state for this step using cyclopentadienone iron carbonyl complexes.[159] The energy span for the bifunctional pathway is defined by **A** (turn over determining intermediate) and **TSBC** (turn over determining transition state), and amounts to 29 kcal mol^{-1}.[160] This is somewhat higher than the experimentally determined value for Gibbs free energy of activation (24 kcal mol^{-1}) (see, Supporting Information).[161] The difference can be attributed to the absence of explicit treatment of solvent in these computations.

In addition to the bifunctional mechanism discussed above, we also studied the likelihood of an inner-sphere *β*-H elimination pathway. The formation of a metal-hydride species via *β*–H elimination has a much higher Gibbs free energy barrier of 45 kcal mol^{-1}, hence, this pathway is discarded. Collectively, DFT results support the role of proton-responsive unit, which is in accordance with the significantly reduced activity observed with catalyst **3** where the proton-responsive unit is absent.

Conclusion

Herein we report the synthesis of a dearomatized Cp*Ir(III) compound **1** bearing a newly designed proton-responsive pyridyl(benzamide)-functionalized NHC ligand. The corresponding aromatized compound **2** was accessible by the protonation of **1**. The protonation of **1** was studied by ^{1}H NMR and UV-vis spectroscopy. The compound **1** exhibits a high catalytic activity for the alkylation of ketones and secondary alcohols using primary alcohols, synthesis of quinolines by annulation reaction using 2-amino-benzyl alcohol with various ketones, and selective alkylation of pregnenolone and testosterone. The control experiments, deuterated labeling and DFT studies support the importance of proton-responsive unit for hydrogen management during a catalytic process. We are currently exploring the potential of this new ligand scaffold in other transformations.

Experimental Section

General Experimental Details. The reactions with metal complexes were carried out under an atmosphere of purified nitrogen using standard Schlenk–vessel and vacuum line techniques. ^{1}H NMR spectra were obtained on JEOL JNM–LA 500MHz and JEOL JNM–LA 400MHz spectrometers. ^{1}H NMR chemical shifts were referenced to the residual hydrogen signal of the deuterated solvents. The chemical shift is given as dimensionless δ values and is frequency referenced relative to TMS for ^{1}H and ^{13}C NMR spectroscopy. The elemental analyses were performed on a Thermoquest EA1110 CHNS/O analyzer. The crystallized compounds were washed several times with dry diethyl ether, powdered and dried under vacuum for at least 48 h prior to elemental analysis. GC–MS experiments were performed on an Agilent 7890A GC and 5975C MS system. Infrared spectra were recorded in the range 4000–400 cm^{-1} on a Vertex 70 Bruker spectrophotometer on KBr pellets. ESI–MS were recorded on a Waters Micromass Quattro Micro triple-quadruplet mass spectrometer. UV–visible spectra were recorded using a JASCO V–670 UV/vis absorption spectrophotometer.

Materials. Solvents were dried by conventional methods, distilled under nitrogen and deoxygenated prior to use. $IrCl_3{\cdot}xH_2O$ was purchased from Arora Matthey, India. 2-amino-6-bromopyridine was purchased from Sigma-Aldrich. $[Cp^*IrCl_2]_2$ was prepared using a literature procedure.[162]

X-ray data collections and refinement. Single-crystal X-ray studies were performed on a CCD Bruker SMART APEX diffractometer equipped with an Oxford Instruments low-temperature attachment. Data were collected at 100(2) K using graphite monochromatic Mo Kα radiation (λ_α = 0.71073 Å). The frames were indexed, integrated, and scaled using SMART and SAINT software packages,[163] and the data were corrected for absorption using SADABS program.[164] The structures were solved and refined with SHELX[165] and OLEX2[166] suites of programs, while additional crystallographic calculations were performed by PLATON program.[167] All hydrogen atoms were included in the final stages of the refinement and were refined with a typical “riding model”. The crystallographic figures have been generated using Diamond 3.1e software.[168] CCDC numbers 2015689-2015692 contain supplementary crystallographic data for all the compounds. These data can be obtained free of charge from the Cambridge Crystallographic Data Centre via www.ccdc.cam.ac.uk/data_request/cif.

Computational details. Density functional theory (DFT) based calculations were performed using Gaussian 16 program package.[169] The alkylation of acetophenone using benzyl alcohol at 130 °C in toluene was used as a model reaction. Geometry optimizations of minima and transition states were performed using GEDIIS (energy represented direct inversion in the iterative subspace for geometry optimization) approach as implemented in Gaussian 16. The density functional used here is M06 hybrid meta-GGA functional.[153] LanL2DZ basis set with effective core potentials[154] was employed for iridium and 6-31+G(d,p) basis set was employed for other elements.[155,156] Normal mode analysis was performed to ascertain the nature of the stationary state points on the potential energy surface. The optimized transition state structures were characterized by the presence of a single imaginary mode and the minima by the absence of such a mode. Solvent corrections to the energies were computed by performing single point calculations on the optimized geometries in gas phase using SMD implicit solvent model with toluene as the solvent. The Gibbs free energies were then computed at 403.15 K and the computed free energy values include both zero-point correction and thermal correction to enthalpy and entropy to the total electronic energy.

Synthesis of 1. In a flame-dried Schlenk flask, $[\mathbf{L^1}H_2]I$ (60 mg, 0.0148 mmol), Ag_2O (33 mg, 0.0148 mmol) and $[Cp^*IrCl_2]_2$ (59 mg, 0.0739 mmol) were dissolved in 15 mL of dichloromethane and stirred at room temperature in the absence of light for 12 h under N_2 atmosphere. The resulting solution was filtered through a pad of celite. Then, the solution was concentrated under reduced pressure and 10 mL of hexane was added to induce precipitation. After the supernatant was discarded through cannula filtration, the precipitate was again washed with hexane (3 × 10 mL) and dried under vacuum. X-ray quality crystals were grown by layering hexane onto a saturated dichloromethane solution of **1** inside an 8 mm o.d. vacuum-sealed glass tube. Yield: 54 mg (90%). ESI–MS, m/z: 605.2737 (z = 1), $[\mathbf{1} - Cl]^+$. ^{1}H NMR (500 MHz, $CDCl_3$, 292 K): δ 8.44 (d, J = 5.15 Hz, 2H), 7.86 (d, J = 10 Hz, 1H), 7.46 (s, 1H), 7.36 (m, 4H), 707 (s, 1H), 6.53 (d, J = 8.6 Hz, 1H), 3.92 (s, 3H), 1.64 (s, 15H). ^{13}C NMR (100 MHz, $CDCl_3$, 292 K): δ 173.1, 166.4, 164.8, 149.8, 149.4, 140.4, 137.2, 129.9, 127.3, 123.8, 116.7, 116.3, 96.1, 91.6, 37.1, 9.8 ppm. IR (KBr) data (cm^{-1}): *ν*(CO): 1618 (s). Anal. Calcd. for $C_{26}H_{28}ClIrN_4O$: C, 48.73; H, 4.40; N, 8.74. Found: C, 48.53; H, 4.31; N, 8.61.

Synthesis of 2. Complex **1** (60 mg, 0.0937 mmol) was dissolved in 15 mL of THF and 1 equivalent (0.0110 mL) of HBF_4 (HBF_4 in ether) was added. The reaction mixture was stirred at room temperature for 2 h under N_2 atmosphere. The solution was concentrated under reduced pressure and 10 mL of diethyl ether was added to induce precipitation.

After the supernatant was discarded through cannula filtration, the precipitate was again washed with diethyl ether (3 × 10 mL) and dried under vacuum. Suitable X-ray quality crystals were grown by layering petroleum ether onto a saturated dichloromethane solution of **2** inside an 8 mm o.d. vacuum–sealed glass tube. Yield: 45 mg (70%). ESI–MS, m/z: 641.1579 (z = 1), $[\mathbf{2} - BF_4]^+$. ^{1}H NMR (500 MHz, CD_3CN, 292 K): δ 10.08 (s, 1H), 8.29 (d, J = 8.30 Hz, 1H), 8.17 (t, J = 8.22 Hz, 1H), 8.08 (d, J = 7.15 Hz, 1H), 7.89 (d, J = 2.25 Hz, 3H), 7.73 (t, J = 7.31 Hz, 1H), 7.44 (d, J = 2.30 Hz, 1H), 4.01 (s, 3H), 1.51 (s, 15H). ^{13}C NMR (125 MHz, CD_3CN, 292 K): δ 166.5, 164.8, 152.7, 151.0, 144.0, 133.7, 129.3, 127.8, 125.7, 118.7, 117.3, 114.0, 107.1, 93.3, 37.6, 8.6 ppm. IR (KBr) data (cm^{-1}): *ν*(CO): 1694 (s), *ν*(NH): 3306 (s). Anal. Calcd. for $C_{26}H_{29}ClIrN_4OBF_4$: C, 42.84; H, 4.01; N, 7.69. Found: C, 42.78; H, 3.99; N, 7.62.

Synthesis 3. Following a synthetic procedure similar to that described for **1**, the reaction of $[\mathbf{L^2}H]PF_6$ (50 mg, 0.163 mmol), Ag_2O (37.7 mg, 0.163 mmol) and $[Cp^*IrCl_2]_2$ (65.3 mg, 0.0819 mmol) in 15 mL of acetonitrile afforded complex **3**. Yield: 40 mg (80%). ESI-MS, m/z: 522.1224 (z = 1), $[\mathbf{3} - PF_6]^+$. ^{1}H NMR (400 MHz, DMSO–d_6, 292 K): δ 8.68 (d, J = 5.52 Hz 1H), 8.43 (d, J = 1.92 Hz, 1H), 8.25 (t, J = 6.1 Hz, 2H), 7.77 (d, J = 1.82 Hz, 1H), 3.92 (s, 3H), 1.72 (s, 15H). ^{13}C NMR (100 MHz, DMSO-d_6, 292 K): δ 166.3, 152.7, 151.6, 142.9, 126.4, 124.7, 117.7, 112.8, 92.2, 37.6, 9.4 ppm. Anal. Calcd for $C_{19}H_{24}N_3ClIrPF_6$: C, 34.17; H, 3.62; N, 6.29. Found: C, 34.14; H, 3.58; N, 6.25.

UV–vis and NMR Monitoring of Protonation of 1

(a) UV–vis Study. The stock solutions of complex **1** (1.0 mM) and trifluoroacetic acid (CF_3CO_2H) (0.33 mM) were prepared in acetonitrile. Then 120 µL of the stock solution of **1** was taken in a quartz cuvette and diluted to 2.2 mL. This solution was titrated gradually by stepwise addition of 30 µL stock solution of CF_3CO_2H. The titration was monitored by UV–vis spectroscopy, which confirmed the protonation of **1**. (b) ^{1}H NMR Study. To a $CDCl_3$ solution (0.5 mL) of complex **1** (5 mg, 0.015 M), 0.2 equivalent of trifluoroacetic acid (CF_3CO_2H) (0.1 µL, 0.015 M solution in 0.1 mL $CDCl_3$, 20 µL) was added in an NMR tube and ^{1}H NMR spectrum was recorded at room temperature. The same amount of CF_3CO_2H was added stepwise until the full conversion of complex **1** to the aromatized complex was achieved as monitored by ^{1}H NMR spectroscopy.

General Procedure for *α*–alkylation of Ketone with Primary Alcohol. A stock solution was prepared by dissolving complex **1** (5 mg, 7.81×10^{-3} mmol) in 3 mL acetonitrile. The required amount of the stock solution (0.05 mol%) was taken in an oven-dried 15 mL reaction vessel, equipped with a magnetic stir bar and acetonitrile was evaporated under reduced pressure. Next, ketone (4.16 mmol), primary alcohol (4.16 mmol) and KOH (10 mol%) were added. After adding 5 mL dry toluene, the vessel was heated at 130 °C in an oil bath for 30 min. The reaction mixture was cooled, diluted with ethyl acetate (EtOAc), passed through a short column of silica and subjected to GC-MS analysis using dodecane as an internal standard to determine yield. The solvent was evaporated under reduced pressure and the residue was purified by column chromatography using silica (hexane/EtOAc). The isolated product was characterized by NMR spectroscopy.

General Procedure for *β*−Alkylation of Secondary Alcohols with Primary Alcohols. The catalyst (0.05 mol%) was added as described for α–alkylation, followed by the addition of secondary alcohol (4.16 mmol), primary alcohol (4.16 mmol), KOH (10 mol%) and 5 mL dry toluene. Then the mixture was heated at 130 °C in an oil bath for 30 min. The reaction mixture was cooled, diluted with EtOAc, passed through a short column of silica and subjected to GC-MS analysis using dodecane as an internal standard to determine yield. The solvent was evaporated under reduced pressure and the residue was purified by column chromatography using silica (hexane/EtOAc). The isolated product was characterized by NMR spectroscopy.

General Procedure for Quinoline Synthesis. The catalyst (0.05 mol%), 2-aminobenzyl alcohol (4.16 mmol), ketone (4.16 mmol), KOH (10 mol%) and 5 mL dry toluene were taken in a 15 mL reaction vessel as described for alkylation reactions. The vessel was heated at 130 °C in an oil bath for 12 h. Then, the reaction mixture was cooled, diluted with EtOAc, passed through a short column of silica and subjected to GC–MS analysis using dodecane as an internal standard to determine yield. The solvent was evaporated under reduced pressure and the residue was purified by column chromatography using silica (hexane/EtOAc). The isolated product was characterized by NMR spectroscopy.

General Procedure for Synthesis of Lactones. The catalyst (0.05 mol%), diol (4.16 mmol), KOH (10 mol%) and 5 mL dry toluene were taken in a 15 mL reaction vessel and heated at 130 °C in an oil bath for 12 h. The reaction mixture was cooled, diluted with EtOAc, passed through a short column of silica and subjected to GC–MS analysis using dodecane as an internal standard to determine yield. The solvent was evaporated under reduced pressure and the residue was purified by column chromatography using silica (hexane/EtOAc). The isolated product was characterized by NMR spectroscopy.

Acknowledgements

We thank the anonymous reviewers for useful suggestions. Financial support from the Science and Engineering Research Board (SERB) is gratefully acknowledged. J.K.B. thanks SERB, India, for a J. C. Bose fellowship. M.K., K.P and A.B thank the CSIR (India), UGC (India), and IIT Kanpur for fellowships, respectively. N.U.D.R. thanks IIT Kanpur for a post-doctoral fellowship. SK thanks the department of science and technology (DST), India for an INSPIRE faculty fellowship and IISER Thiruvananthapuram for providing the HPC facilities.

Keywords: • Proton-Responsive Ligand • Metal-Ligand Cooperation • Borrowing-Hydrogen • Hydrogen transfer • Homogeneous Catalysis • Reaction Mechanism

[1] S. Kuwata, T. Ikariya, *Chem. Commun.* **2014**, *50*, 14290–14300.
[2] J. R. Khusnutdinova, D. Milstein, *Angew. Chem. Int. Ed.* **2015**, *54*, 12236–12273.
[3] L. Wang, R. Kanega, H. Kawanami, Y. Himeda, *Chem. Rec.* **2017**, *17*, 1071–1094.
[4] N. Onishi, M. Iguchi, X. Yang, R. Kanega, H. Kawanami, Q. Xu, Y. Himeda, *Adv. Energy Mater.* **2019**, *9*, 1801275.
[5] H. Li, T. P. Gonçalves, D. Lupp, K. W. Huang, *ACS Catal.* **2019**, *9*, 1619–1629.
[6] K. I. Fujita, *Bull. Chem. Soc. Jpn.* **2019**, *92*, 344–351.
[7] S. Kuwata, T. Ikariya, *Chem. Eur. J.* **2011**, *17*, 3542–3556.
[8] S. Semwal, J. Choudhury, *Angew. Chem. Int. Ed.* **2017**, *56*, 5556–5560.
[9] F. E. Hahn, *ChemCatChem* **2013**, *5*, 419–430.
[10] E. Peris, *Chem. Rev.* **2018**, *118*, 9988–10031.
[11] B. Maji, J. Choudhury, *Chem. Commun.* **2019**, *55*, 4574–4577.
[12] A. Bartoszewicz, R. Marcos, S. Sahoo, A. K. Inge, X. Zou, B. Martín-Matute, *Chem. Eur. J.* **2012**, *18*, 14510–14519.
[13] T. Yan, B. L. Feringa, K. Barta, *Nat. Commun.* **2014**, *5*, 5602.
[14] Y. Ai, P. Liu, R. Liang, Y. Liu, F. Li, *New J. Chem.* **2019**, *43*, 10755–10762.
[15] A. Kaithal, P. van Bonn, M. Hölscher, W. Leitner, *Angew. Chem. Int. Ed.* **2020**, *59*, 215–220.

[16] C. Seck, M. D. Mbaye, S. Gaillard, J. L. Renaud, *Adv. Synth. Catal.* **2018**, *360*, 4640–4645.
[17] A. Kumar, S. Semwal, J. Choudhury, *Chem. Eur. J.* **2021**, chem.202004499.
[18] K.-W. Huang, T. P. Goncalves, I. Dutta, *Chem. Commun.* **2021**, *57*, 3070–3082.
[19] B. Chatterjee, W. C. Chang, S. Jena, C. Werlé, *ACS Catal.* **2020**, *10*, 14024–14055.
[20] M. R. Elsby, R. T. Baker, *Chem. Soc. Rev.* **2020**, *49*, 8933–8987.
[21] R. H. Morris, *Chem. Rev.* **2016**, *116*, 8588–8654.
[22] M. Rakowski Dubois, D. L. Dubois, *Chem. Soc. Rev.* **2009**, *38*, 62–72.
[23] L. V. A. Hale, N. K. Szymczak, *ACS Catal.* **2018**, *8*, 6446–6461.
[24] O. Eisenstein, R. H. Crabtree, *New J. Chem.* **2013**, *37*, 21–27.
[25] K. I. Fujita, T. Yoshida, Y. Imori, R. Yamaguchi, *Org. Lett.* **2011**, *13*, 2278–2281.
[26] K. I. Fujita, N. Tanino, R. Yamaguchi, *Org. Lett.* **2007**, *9*, 109–111.
[27] K. I. Fujita, R. Tamura, Y. Tanaka, M. Yoshida, M. Onoda, R. Yamaguchi, *ACS Catal.* **2017**, *7*, 7226–7230.
[28] Y. Suna, M. Z. Ertem, W. H. Wang, H. Kambayashi, Y. Manaka, J. T. Muckerman, E. Fujita, Y. Himeda, *Organometallics* **2014**, *33*, 6519–6530.
[29] R. Kawahara, K. I. Fujita, R. Yamaguchi, *J. Am. Chem. Soc.* **2012**, *134*, 3643–3646.
[30] K. I. Fujita, T. Wada, T. Shiraishi, *Angew. Chem. Int. Ed.* **2017**, *56*, 10886–10889.
[31] K. I. Fujita, Y. Tanaka, M. Kobayashi, R. Yamaguchi, *J. Am. Chem. Soc.* **2014**, *136*, 4829–4832.
[32] R. Kawahara, K. I. Fujita, R. Yamaguchi, *Angew. Chem. Int. Ed.* **2012**, *51*, 12790–12794.
[33] J. F. Hull, Y. Himeda, W. H. Wang, B. Hashiguchi, R. Periana, D. J. Szalda, J. T. Muckerman, E. Fujita, *Nat. Chem.* **2012**, *4*, 383–388.
[34] L. Wang, N. Onishi, K. Murata, T. Hirose, J. T. Muckerman, E. Fujita, Y. Himeda, *ChemSusChem* **2017**, *10*, 1071–1075.
[35] Y. Manaka, W. H. Wang, Y. Suna, H. Kambayashi, J. T. Muckerman, E. Fujita, Y. Himeda, *Catal. Sci. Technol.* **2014**, *4*, 34–37.
[36] W. H. Wang, J. T. Muckerman, E. Fujita, Y. Himeda, *ACS Catal.* **2013**, *3*, 856–860.
[37] N. Onishi, S. Xu, Y. Manaka, Y. Suna, W. H. Wang, J. T. Muckerman, E. Fujita, Y. Himeda, *Inorg. Chem.* **2015**, *54*, 5114–5123.
[38] F. Li, J. Ma, N. Wang, *J. Org. Chem.* **2014**, *79*, 10447–10455.
[39] P. Qu, C. Sun, J. Ma, F. Li, *Adv. Synth. Catal.* **2014**, *356*, 447–459.
[40] M. Huang, Y. Li, J. Liu, X. B. Lan, Y. Liu, C. Zhao, Z. Ke, *Green Chem.* **2019**, *21*, 219–224.
[41] P. Pandey, P. Daw, N. U. Din Reshi, K. R. Ehmann, M. Hölscher, W. Leitner, J. K. Bera, *Organometallics* **2020**, *39*, 3849–3863.
[42] M. Mondal, T. K. Ranjeesh, S. K. Gupta, J. Choudhury, *Dalt. Trans.* **2014**, *43*, 9356–9362.
[43] L. Benhamou, V. César, H. Gornitzka, N. Lugan, G. Lavigne, *Chem. Commun.* **2009**, 4720–4722.
[44] J. Zhang, G. Leitus, Y. Ben-David, D. Milstein, *J. Am. Chem. Soc.* **2005**, *127*, 10840–10841.
[45] C. Gunanathan, D. Milstein, *Chem. Rev.* **2014**, *114*, 12024–12087.
[46] T. Zell, D. Milstein, *Acc. Chem. Res.* **2015**, *48*, 1979–1994.
[47] G. Van Koten, *Organometallic Pincer Chemistry*, Springer Berlin Heidelberg, Berlin, Heidelberg, **2013**.
[48] D. Milstein, in *Top. Catal.*, **2010**, pp. 915–923.
[49] C. Gunanathan, D. Milstein, in *Top. Organomet. Chem.*, Springer, Berlin, Heidelberg, **2011**, pp. 55–84.
[50] M. E. van der Boom, D. Milstein, *Chem. Rev.* **2003**, *103*, 1759–1792.
[51] E. Fogler, E. Balaraman, Y. Ben-David, G. Leitus, L. J. W. Shimon, D. Milstein, *Organometallics* **2011**, *30*, 3826–3833.
[52] U. K. Das, Y. Ben-David, Y. Diskin-Posner, D. Milstein, *Angew. Chem. Int. Ed.* **2018**, *57*, 2179–2182.
[53] L. P. He, T. Chen, D. Gong, Z. Lai, K. W. Huang, *Organometallics* **2012**, *31*, 5208–5211.
[54] H. Li, B. Zheng, K.-W. Huang, *Coord. Chem. Rev.* **2015**, *293–294*, 116–138.
[55] Y. Pan, C. L. Pan, Y. Zhang, H. Li, S. Min, X. Guo, B. Zheng, H. Chen, A. Anders, Z. Lai, J. Zheng, K. W. Huang, *Chem. Asian J.* **2016**, *11*, 1357–1360.
[56] H. Li, T. P. Gonçalves, Q. Zhao, D. Gong, Z. Lai, Z. Wang, J. Zheng, K. W. Huang, *Chem. Commun.* **2018**, *54*, 11395–11398.
[57] T. Chen, H. Li, S. Qu, B. Zheng, L. He, Z. Lai, Z. X. Wang, K. W. Huang, *Organometallics* **2014**, *33*, 4152–4155.
[58] D. Gong, W. Liu, T. Chen, Z.-R. Chen, K.-W. Huang, *J. Mol. Catal. A Chem.* **2014**, *395*, 100–107.
[59] H. Li, Y. Wang, Z. Lai, K. W. Huang, *ACS Catal.* **2017**, *7*, 4446–4450.
[60] Y. Wang, B. Zheng, Y. Pan, C. Pan, L. He, K. W. Huang, *Dalt. Trans.* **2015**, *44*, 15111–15115.
[61] S. Qu, Y. Dang, C. Song, M. Wen, K. W. Huang, Z. X. Wang, *J. Am. Chem. Soc.* **2014**, *136*, 4974–4991.
[62] C. Yao, T. Zhang, C. Zhou, K. W. Huang, *Dalt. Trans.* **2019**, *48*, 12817–12821.
[63] Y. Pan, C. Guan, H. Li, P. Chakraborty, C. Zhou, K. W. Huang, *Dalt. Trans.* **2019**, *48*, 12812–12816.
[64] D. Lupp, K.-W. Huang, *Organometallics* **2020**, *39*, 18–24.
[65] T. Chen, L. P. He, D. Gong, L. Yang, X. Miao, J. Eppinger, K. W. Huang, *Tetrahedron Lett.* **2012**, *53*, 4409–4412.
[66] L. P. He, T. Chen, D. X. Xue, M. Eddaoudi, K. W. Huang, *J. Organomet. Chem.* **2012**, *700*, 202–206.
[67] G. Zeng, T. Chen, L. He, I. Pinnau, Z. Lai, K. W. Huang, *Chem. Eur. J.* **2012**, *18*, 15940–15943.
[68] F. Bertini, M. Glatz, N. Gorgas, B. Stöger, M. Peruzzini, L. F. Veiros, K. Kirchner, L. Gonsalvi, *Chem. Sci.* **2017**, *8*, 5024–5029.
[69] F. Bertini, N. Gorgas, B. Stöger, M. Peruzzini, L. F. Veiros, K. Kirchner, L. Gonsalvi, *ACS Catal.* **2016**, *6*, 2889–2893.
[70] B. Bichler, C. Holzhacker, B. Stöger, M. Puchberger, L. F. Veiros, K. Kirchner, *Organometallics* **2013**, *32*, 4114–4121.
[71] N. Gorgas, K. Kirchner, *Acc. Chem. Res.* **2018**, *51*, 1558–1569.
[72] M. Glatz, B. Stöger, D. Himmelbauer, L. F. Veiros, K. Kirchner, *ACS Catal.* **2018**, *8*, 4009–4016.
[73] M. Mastalir, G. Tomsu, E. Pittenauer, G. Allmaier, K. Kirchner, *Org. Lett.* **2016**, *18*, 3462–3465.
[74] N. Gorgas, L. G. Alves, B. Stöger, A. M. Martins, L. F. Veiros, K. Kirchner, *J. Am. Chem. Soc.* **2017**, *139*, 8130–8133.
[75] F. Bertini, M. Glatz, B. Stöger, M. Peruzzini, L. F. Veiros, K. Kirchner, L. Gonsalvi, *ACS Catal.* **2019**, *9*, 632–639.
[76] D. Benito-Garagorri, E. Becker, J. Wiedermann, W. Lackner, M. Pollak, K. Mereiter, J. Kisala, K. Kirchner, *Organometallics* **2006**, *25*, 1900–1913.
[77] D. Benito-Garagorri, K. Kirchner, *Acc. Chem. Res.* **2008**, *41*, 201–

213.

[78] N. Gorgas, B. Stöger, L. F. Veiros, E. Pittenauer, G. Allmaier, K. Kirchner, *Organometallics* **2014**, *33*, 6905–6914.

[79] M. Mastalir, B. Stöger, E. Pittenauer, M. Puchberger, G. Allmaier, K. Kirchner, *Adv. Synth. Catal.* **2016**, *358*, 3824–3831.

[80] M. Mastalir, M. Glatz, N. Gorgas, B. Stöger, E. Pittenauer, G. Allmaier, L. F. Veiros, K. Kirchner, *Chem. Eur. J.* **2016**, *22*, 12316–12320.

[81] M. Mastalir, M. Glatz, E. Pittenauer, G. Allmaier, K. Kirchner, *J. Am. Chem. Soc.* **2016**, *138*, 15543–15546.

[82] A. Bruneau-Voisine, D. Wang, T. Roisnel, C. Darcel, J.-B. Sortais, *Catal. Commun.* **2017**, *92*, 1–4.

[83] A. Bruneau-Voisine, D. Wang, V. Dorcet, T. Roisnel, C. Darcel, J.-B. Sortais, *J. Catal.* **2017**, *347*, 57–62.

[84] N. Deibl, R. Kempe, *Angew. Chem. Int. Ed.* **2017**, *56*, 1663–1666.

[85] F. Kallmeier, T. Irrgang, T. Dietel, R. Kempe, *Angew. Chem. Int. Ed.* **2016**, *55*, 11806–11809.

[86] F. Kallmeier, B. Dudziec, T. Irrgang, R. Kempe, *Angew. Chem. Int. Ed.* **2017**, *56*, 7261–7265.

[87] F. Freitag, T. Irrgang, R. Kempe, *Chem. Eur. J.* **2017**, *23*, 12110–12113.

[88] S. Rösler, M. Ertl, T. Irrgang, R. Kempe, *Angew. Chem. Int. Ed.* **2015**, *54*, 15046–15050.

[89] G. Zhang, T. Irrgang, T. Dietel, F. Kallmeier, R. Kempe, *Angew. Chem. Int. Ed.* **2018**, *57*, 9131–9135.

[90] M. Schlagbauer, F. Kallmeier, T. Irrgang, R. Kempe, *Angew. Chem. Int. Ed.* **2020**, *59*, 1485–1490.

[91] S. Michlik, R. Kempe, *Nat. Chem.* **2013**, *5*, 140–144.

[92] G. Zeng, S. Sakaki, K. I. Fujita, H. Sano, R. Yamaguchi, *ACS Catal.* **2014**, *4*, 1010–1020.

[93] T. Irrgang, R. Kempe, *Chem. Rev.* **2019**, *119*, 2524–2549.

[94] C. Zhang, J. P. Zhao, B. Hu, J. Shi, D. Chen, *Organometallics* **2019**, *38*, 654–664.

[95] H. Lundberg, H. Adolfsson, *Synth.* **2016**, *48*, 644–652.

[96] Y. Obora, *ACS Catal.* **2014**, *4*, 3972–3981.

[97] A. J. A. Watson, J. M. J. Williams, *Science* **2010**, *329*, 635–636.

[98] M. H. S. A. Hamid, P. A. Slatford, J. M. J. Williams, *Adv. Synth. Catal.* **2007**, *349*, 1555–1575.

[99] F. Huang, Z. Liu, Z. Yu, *Angew. Chem. Int. Ed.* **2016**, *55*, 862–875.

[100] A. Corma, J. Navas, M. J. Sabater, *Chem. Rev.* **2018**, *118*, 1410–1459.

[101] M. Iglesias, L. A. Oro, *Chem. Soc. Rev.* **2018**, *47*, 2772–2808.

[102] B. G. Reed-Berendt, K. Polidano, L. C. Morrill, *Org. Biomol. Chem.* **2019**, *17*, 1595–1607.

[103] T. D. Nixon, M. K. Whittlesey, J. M. J. J. Williams, *Dalt. Trans.* **2009**, 753–762.

[104] T. Liu, L. Wang, K. Wu, Z. Yu, *ACS Catal.* **2018**, *8*, 7201–7207.

[105] D. Wang, R. T. McBurney, I. Pernik, B. A. Messerle, *Dalt. Trans.* **2019**, *48*, 13989–13999.

[106] B. C. Roy, K. Chakrabarti, S. Shee, S. Paul, S. Kundu, *Chem. Eur. J.* **2016**, *22*, 18147–18155.

[107] O. El-Sepelgy, E. Matador, A. Brzozowska, M. Rueping, *ChemSusChem* **2019**, *12*, 3099–3102.

[108] X. N. Cao, X. M. Wan, F. L. Yang, K. Li, X. Q. Hao, T. Shao, X. Zhu, M. P. Song, *J. Org. Chem.* **2018**, *83*, 3657–3668.

[109] K. Chakrabarti, B. Paul, M. Maji, B. C. Roy, S. Shee, S. Kundu, *Org. Biomol. Chem.* **2016**, *14*, 10988–10997.

[110] L. Bettoni, S. Gaillard, J. L. Renaud, *Org. Lett.* **2020**, *22*, 2064–2069.

[111] J. Das, K. Singh, M. Vellakkaran, D. Banerjee, *Org. Lett.* **2018**, *20*, 5587–5591.

[112] X. B. Lan, Z. Ye, J. Liu, M. Huang, Y. Shao, X. Cai, Y. Liu, Z. Ke, *ChemSusChem* **2020**, *13*, 2557–2563.

[113] S. Shee, B. Paul, D. Panja, B. C. Roy, K. Chakrabarti, K. Ganguli, A. Das, G. K. Das, S. Kundu, *Adv. Synth. Catal.* **2017**, *359*, 3888–3893.

[114] S. Genç, B. Arslan, S. Gülcemal, S. Günnaz, B. Çetinkaya, D. Gülcemal, *J. Org. Chem.* **2019**, *84*, 6286–6297.

[115] G. Guillena, D. J. Ramón, M. Yus, *Angew. Chemie Int. Ed.* **2007**, *46*, 2358–2364.

[116] X. B. Lan, Z. Ye, M. Huang, J. Liu, Y. Liu, Z. Ke, *Org. Lett.* **2019**, *21*, 8065–8070.

[117] J. Das, M. Vellakkaran, D. Banerjee, *J. Org. Chem.* **2019**, *84*, 769–779.

[118] P. Piehl, R. Amuso, E. Alberico, H. Junge, B. Gabriele, H. Neumann, M. Beller, *Chem. Eur. J.* **2020**, *26*, 6050–6055.

[119] S. Chakraborty, P. Daw, Y. Ben David, D. Milstein, *ACS Catal.* **2018**, *8*, 10300–10305.

[120] L. M. Kabadwal, J. Das, D. Banerjee, *Chem. Commun.* **2018**, *54*, 14069–14072.

[121] M. Peña-López, P. Piehl, S. Elangovan, H. Neumann, M. Beller, *Angew. Chem. Int. Ed.* **2016**, *55*, 14967–14971.

[122] S. Genç, S. Günnaz, B. Çetinkaya, S. Gülcemal, D. Gülcemal, *J. Org. Chem.* **2018**, *83*, 2875–2881.

[123] S. Movassaghi, S. Singh, A. Mansur, K. K. H. Tong, M. Hanif, H. U. Holtkamp, T. Söhnel, S. M. F. Jamieson, C. G. Hartinger, *Organometallics* **2018**, *37*, 1575–1584.

[124] Z. G. Specht, D. B. Grotjahn, C. E. Moore, A. L. Rheingold, *Organometallics* **2013**, *32*, 6400–6409.

[125] X. Q. Xiao, G. X. Jin, *J. Organomet. Chem.* **2008**, *693*, 3363–3368.

[126] S. Klein, W. G. Dougherty, W. S. Kassel, T. J. Dudley, J. J. Paul, *Inorg. Chem.* **2011**, *50*, 2754–2763.

[127] A. M. W. Cargill Thompson, M. C. C. Smailes, J. C. Jeffery, M. D. Ward, *J. Chem. Soc. - Dalt. Trans.* **1997**, *9*, 737–743.

[128] J. Depasquale, I. Nieto, L. E. Reuther, C. J. Herbst-Gervasoni, J. J. Paul, V. Mochalin, M. Zeller, C. M. Thomas, A. W. Addison, E. T. Papish, *Inorg. Chem.* **2013**, *52*, 9175–9183.

[129] Y. M. Badiei, W. H. Wang, J. F. Hull, D. J. Szalda, J. T. Muckerman, Y. Himeda, E. Fujita, *Inorg. Chem.* **2013**, *52*, 12576–12586.

[130] S. Semwal, J. Choudhury, *ACS Catal.* **2016**, *6*, 2424–2428.

[131] R. Corberán, E. Peris, *Organometallics* **2008**, *27*, 1954–1958.

[132] A. Prades, R. Corberán, M. Poyatos, E. Peris, *Chem. Eur. J.* **2008**, *14*, 11474–11479.

[133] A. Prades, R. Corberán, M. Poyatos, E. Peris, *Chem. Eur. J.* **2009**, *15*, 4610–4613.

[134] T. P. Vispute, H. Zhang, A. Sanna, R. Xiao, G. W. Huber, *Science* **2010**, *330*, 1222–1227.

[135] P. Chakraborty, M. K. Gangwar, B. Emayavaramban, E. Manoury, R. Poli, B. Sundararaju, *ChemSusChem* **2019**, *12*, 3463–3467.

[136] C. Meng, J. Xu, Y. Tang, Y. Ai, F. Li, *New J. Chem.* **2019**, *43*, 14057–14065.

[137] S. Waiba, S. K. Jana, A. Jati, A. Jana, B. Maji, *Chem. Commun.* **2020**, *56*, 8376–8379.

[138] S. Thiyagarajan, R. Vijaya Sankar, C. Gunanathan, *Org. Lett.* **2020**, *22*, 7879–7884.

[139] Q. Wang, K. Wu, Z. Yu, *Organometallics* **2016**, *35*, 1251–1256.

[140] A. A. Joshi, C. L. Viswanathan, *Bioorganic Med. Chem. Lett.* **2006**, *16*, 2613–2617.

[141] S. Mukherjee, M. Pal, *Curr. Med. Chem.* **2013**, *20*, 4386–4410.

[142] S. Vandekerckhove, M. D'Hooghe, *Bioorganic Med. Chem.* **2015**, *23*, 5098–5119.

[143] J. Marco-Contelles, R. León, M. G. López, A. G. García, M. Villarroya, *Eur. J. Med. Chem.* **2006**, *41*, 1464–1469.

[144] P. Zhang, Y. Ye, Y. Qian, B. Yin, J. Zhao, S. Zhu, L. Zhang, M. Yan, *CNS Neurol. Disord. Drug Targets* **2017**, *16*, 724–736.

[145] J. Qin, M. Wu, S. Yu, X. Gao, J. Zhang, X. Dong, J. Ji, Y. Zhang, L. Zhou, Q. Zhang, F. Ding, *Toxicol. Lett.* **2015**, *238*, 70–82.

[146] Y. Tang, R. I. L. Meador, C. T. Malinchak, E. E. Harrison, K. A. McCaskey, M. C. Hempel, T. W. Funk, *J. Org. Chem.* **2020**, *85*, 1823–1834.

[147] K. I. Fujita, W. Ito, R. Yamaguchi, *ChemCatChem* **2014**, *6*, 109–112.

[148] S. Bi, Y. Y. Jiang, T. T. Liu, S. Y. Tang, B. Hu, P. Liu, *J. Org. Chem.* **2020**, *85*, 12444–12455.

[149] I. Dutta, A. Sarbajna, P. Pandey, S. M. W. Rahaman, K. Singh, J. K. Bera, *Organometallics* **2016**, *35*, 1505–1513.

[150] S. E. Clapham, A. Hadzovic, R. H. Morris, *Coord. Chem. Rev.* **2004**, *248*, 2201–2237.

[151] J. S. M. M. Samec, J.-E. E. Bäckvall, P. G. Andersson, P. Brandt, M. Lemaire, M. Lemaire, J. Park, P. Rigo, P. W. N. M. van Leeuwen, *Chem. Soc. Rev.* **2006**, *35*, 237–248.

[152] O. Pàmies, J.-E. E. Bäckvall, *Chem. Eur. J.* **2001**, *7*, 5052–5058.

[153] Y. Zhao, D. G. Truhlar, *Theor. Chem. Acc.* **2008**, *120*, 215–241.

[154] P. J. Hay, W. R. Wadt, *J. Chem. Phys.* **1985**, *82*, 299–310.

[155] G. A. Petersson, M. A. Al-Laham, *J. Chem. Phys.* **1991**, *94*, 6081–6090.

[156] W. J. Hehre, K. Ditchfield, J. A. Pople, *J. Chem. Phys.* **1972**, *56*, 2257–2261.

[157] K. N. T. Tseng, J. W. Kampf, N. K. Szymczak, *ACS Catal.* **2015**, *5*, 5468–5485.

[158] C. Hou, Z. Zhang, C. Zhao, Z. Ke, *Inorg. Chem.* **2016**, *55*, 6539–6551.

[159] C. Seck, M. D. Mbaye, S. Coufourier, A. Lator, J. F. Lohier, A. Poater, T. R. Ward, S. Gaillard, J. L. Renaud, *ChemCatChem* **2017**, *9*, 4410–4416.

[160] S. Kozuch, S. Shaik, *Acc. Chem. Res.* **2011**, *44*, 101–110.

[161] S. Kozuch, J. M. L. Martin, *ACS Catal.* **2012**, *2*, 2787–2794.

[162] R. G. Ball, W. A. G. Graham, J. K. Hoyano, A. D. McMaster, B. M. Mattson, D. M. Heinekey, B. M. Mattson, S. T. Michel, *Inorg. Chem.* **1990**, *29*, 2023–2025.

[163] SAINT+ Software for CCD Diffractometers, Bruker AXS, Madison, WI, **2000.**

[164] SADABS 2.0, G. M. Sheldrick, **2000**.

[165] SHELXL-2014:Program for Crystal Structure Refinemen, G. M. Sheldrick, University of Gçttingen, Gçttingen (Germany), **2014**.

[166] O. V. Dolomanov, L. J. Bourhis, R. J. Gildea, J. A. K. Howard, H. Puschmann, *J. Appl. Crystallogr.* **2009**, *42*, 339–341.

[167] PLATON, A. L. Spek, University of Utrecht, Utrecht (The Netherlands), **2001.**

[168] Diamond, version 3.1e, K. Bradenburg, Crystal Impact GbR, Bonn (Germany), **2005**.

[169] Gaussian16, Revision C.01, M. J. Frisch, G. W. Trucks, H. B. Schlegel, G. E. Scuseria, M. A. Robb, J. R. Cheeseman, G. Scalmani, V. Barone, B. Mennucci, G. A. Petersson, H. Nakatsuji, M. Caricato, X. Li, H. P. Hratchian, A. F. Izmaylov, J. Bloino, G. Zheng, J. L. Sonnenberg, M. Hada, M. Ehara, K. Toyota, R. Fukuda, J. Hasegawa, M. Ishida, T. Nakajima, Y. Honda, O. Kitao, H. Nakai, T. Vreven, J. A. Montgomery, Jr., J. E. Peralta, F. Ogliaro, M. Bearpark, J. J. Heyd, E. Brothers, K. N. Kudin, V. N. Staroverov, T. Keith, R. Kobayashi J. Normand, K. Raghavachari, A. Rendell, J. C. Burant, S. S. Iyengar, J. Tomasi, M. Cossi, N. Rega, J. M. Millam, M. Klene, J. E. Knox, J. B. Cross V. Bakken, C. Adamo, J. Jaramillo, R. Gomperts, R. E. Stratmann, O. Yazyev, A. J. Austin, R. Cammi, C. Pomelli, J. W. Ochterski, R. L. Martin, K. Morokuma, V. G. Zakrzewski, G. A. Voth, P. Salvador, J. J. Dannenberg, S. Dapprich, A. D. Daniels, O. Farkas, J. B. Foresman, J. V. Ortiz, J. Cioslowski, D. J. Fox.

Entry for the Table of Contents

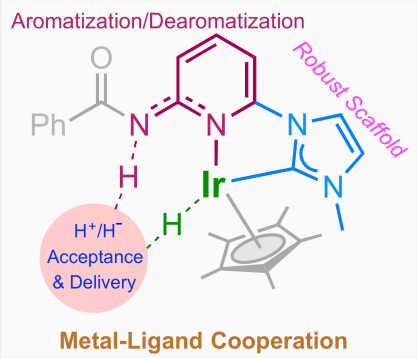

A Cp*Ir(III) complex bearing a pyridyl(benzamide)-functionalized N-heterocyclic carbene (NHC) ligand exhibits aromatization/dearomatization on protonation/deprotonation. The proton-responsive unit of the title compound plays a key role in catalyzing α-alkylation of ketones and β-alkylation of secondary alcohols using primary alcohols via a borrowing-hydrogen pathway.